Nonlinear optical processes at quadrupole polariton resonance in Cu_2O as probed by a Z-scan technique

S. Mani,[1] J. I. Jang,[1,*] and J. B. Ketterson[1,2]

[1]*Department of Physics and Astronomy, Northwestern University, 2145 Sheridan Road, Evanston, Illinois 60208, USA*

[2]*Department of Electrical Engineering and Computer Science, Northwestern University, 2145 Sheridan Road, Evanston, Illinois 60208, USA*

(Received 25 August 2010; revised manuscript received 4 September 2010; published 28 September 2010)

Employing a modified Z-scan technique at 2 K, we monitor not only the fundamental (ω) but also the frequency-doubled (2ω) and tripled (3ω) Z-scan responses in Cu_2O when the input laser frequency ω is tuned to the two-photon quadrupole polariton resonance. The Z-scan response at ω allows us to accurately estimate the absolute number of polaritons generated via two-photon absorption. A striking dip is observed near the 2ω Z-scan focus which basically arises from Auger-type recombination of polaritons. Under high excitation levels, the 3ω Z-scan shows strong third harmonic generation. Based on the nonlinear optical parameters determined, we estimate the experimental polariton density achievable and propose a direction for polariton-based Bose-Einstein condensation in Cu_2O.

DOI: 10.1103/PhysRevB.82.113203 PACS number(s): 71.36.+c, 42.65.−k, 71.35.Lk

Although now commonplace in atomic systems,[1,2] Bose-Einstein condensation (BEC) of excitons in bulk semiconductors has long been a quest, with Cu_2O being a primary candidate historically.[3] Exciton polaritons (hereafter called polaritons) offer an alternative approach and condensation in two-dimensional (2D) quantum-well structures was recently reported where multilayer Bragg mirrors confined the optical components.[4–6] However, even under strong cavity confinement, this "nonequilibrium" polariton BEC lasts for much less than 1 ns, basically due to the short-lived excitonic component undergoing efficient dipole transitions in materials such as GaAs and CdTe.

Decay of the singlet and triplet exciton ground states in Cu_2O is *dipole forbidden* and they have a relatively small effective mass. The corresponding critical BEC density is about 10^{17} cm^{-3} at 2 K, which could be readily achievable using ordinary optical excitation. But exciton BEC turns out to be elusive due to a nonradiative Auger-type recombination that becomes more significant at high density and low temperature.[7]

The long-lived polaritons in Cu_2O may offer an alternative route to BEC; in fact the existence of long-lived polaritons (up to a few nanoseconds) has been firmly established by coherent quantum beat spectroscopy.[8] This much longer lifetime arises from the above noted dipole-forbidden nature of Cu_2O and radiative decay of polaritons occurs primarily via a quadrupole transition. These *quadrupole* polaritons have been actively researched using resonant two-photon absorption (TPA).[9–19] Despite preliminary results indicating suppressed Auger-type loss for polaritons,[13,16] no signature for polariton BEC has been observed in Cu_2O. Also, it has been recently suggested that three-photon excitation[17] and third harmonic generation (THG) (Ref. 20) can affect polariton population dynamics under strong excitation. Considering possible complications caused by these high-order processes, the feasibility of polariton BEC in Cu_2O remains an open question.

In pursuit of this question we have systematically investigated various nonlinear optical processes such as TPA, Auger-type recombination and THG under resonant two-photon excitation (ω=1.016 eV) at 2 K using a Z-scan method. This technique is traditionally utilized to probe the third-order nonlinearity $\chi^{(3)}$ by translating a test sample through the beam waist of a focused Gaussian-laser profile and measuring the corresponding variation of the transmitted beam intensity in the far field.[21,22] In our experiments a train of 30-ps laser pulses from an optical parametric amplifier, pumped by a 10-Hz Nd:YAG laser (355 nm), was spatially filtered using a 100 μm pinhole, insuring transmission of only the TEM_{00} Gaussian mode (see Fig. 1 inset). The incident beam was focused on a d=100-μm-thick (110)-oriented natural-growth Cu_2O crystal in which the relevant selection rules[12,15] were previously confirmed. A lens with a 7.5 cm focal length was mounted on a computer-controlled stage that was translated relative to the window of our optical cryostat, thereby changing the input intensity I as a function of the lens position Z. The change in the far-field image of the transmitted beam with Z was minimized by using a combination of collection lenses prior to entering a photomultiplier tube (PMT). The output of the PMT was fed into a boxcar integrator and read out using a data acquisition system (see Ref. 20 for experimental details). By extending the standard Z-scan method (that only monitors the intensity at ω), we also kept track of the frequency-doubled (2ω) and tripled (3ω) Z-scan outputs to probe the polariton and THG responses using appropriate band-pass filters.

In order to estimate the absolute number of polaritons, it is essential to precisely determine the TPA coefficient β, basically arising from Im $\chi^{(3)}$ at the polariton resonance. Figure 1 plots the normalized ω Z-scan trace (dots), showing nonlinear TPA for 10.4 μJ/pulse. Note that only 0.4% of the incident beam is absorbed at the focus (Z=0). The solid red is a theoretical fit, using Eq. (30) of Ref. 21, to the data with β=0.217 cm/GW and the beam waist of ω_0=15.1 μm at Z=0. This ω_0 is consistent with the Gaussian width σ =0.19 cm of the incident beam through $\sigma/f=\lambda/\pi\omega_0$, where f=7.5 cm and λ=1.22 μm. Unlike conventional band-to-band TPA, at the narrow polariton resonance the effect depends on the spectral width $\Delta\omega$ of the incident laser. In our case of $\Delta\omega \simeq 8$ meV, we found that β=0.217 cm/GW

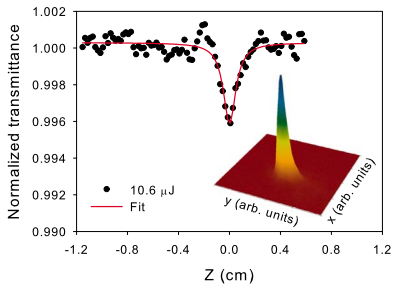

FIG. 1. (Color online) Normalized ω Z-scan for 10.6 μJ/pulse, superimposed by a theoretical fit with β=0.217 cm/GW. Inset: far-field image of the laser profile after spatial filtering taken by a gated intensified CCD camera.

within a 50% uncertainty based on the series of experiments. We also confirmed that the measured β value persists up to 226 μJ/pulse without any evidence for higher order multiphoton absorption.

With β determined, depletion of the fundamental intensity I along the beam path z due to TPA can be calculated and is given by

$$\frac{dI}{dz} = -\beta I^2 \rightarrow I(z;Z,t) = \frac{I_0(Z,t)}{I_0(Z,t)\beta z + 1}, \tag{1}$$

where $I_0(Z,t)$ is the photon flux at the incident sample surface, which is a function of the focusing lens position Z and given by

$$I_0(Z,t) = \frac{2P(t)}{\pi\omega^2(Z)} \rightarrow \frac{2P}{\pi\omega^2(Z)} = \frac{2P}{\pi\omega_0^2(1+Z^2/Z_0^2)}, \tag{2}$$

where $P(t)$ is the input pulse power with a 30-ps Gaussian temporal profile and $Z_0=\pi\omega_0^2/\lambda \simeq 0.06$ cm is the confocal parameter. Since Z-scan yields the time-averaged data, we used the time-integrated pulse power P to evaluate $I_0(Z)$. In Eq. (2), a factor of 2 is correctly introduced for the averaged power of the spatial Gaussian beam. Note that, for a given P, we can continuously vary $I_0(Z)$ more than a factor of 400, simply by translating Z in our Z-scan range $|Z| \leq 1.2$ cm.

Figure 2(a) plots the 2ω Z-scan traces (colored dots) under several excitation levels from 10.4 to 226 μJ/pulse, showing polaritons generated by TPA. Note that we also plot the time-averaged *absolute* number of polaritons using the measured β as explained below. As predicted for TPA in a finite-thickness sample, for a given excitation level, the measured polariton number increases quadratically with the corresponding $I_0(Z)$ as we sweep Z.[23] However, a striking dip-like feature develops in the vicinity of Z=0 as we increase the pulse energy and polariton generation severely saturates at the focus. As an example Fig. 2(b) plots the polariton profiles at Z=−0.4 and 0 cm for 122 μJ/pulse, which clearly shows the reduced polariton number at the focus with no significant spatial broadening. Together with ω Z-scan indicating negligible higher order contributions, this implies that polaritons undergo an Auger-type process at high densities. To check whether any signal was lost due to the finite aperture of the PMT collector, we probed the polariton spatial profile in the far field as a function of Z using a gated intensified charge coupled device (CCD) camera and verified that this mechanism is negligible. (Wide-angle polariton-polariton scattering is expected to conserve the total polariton number.)

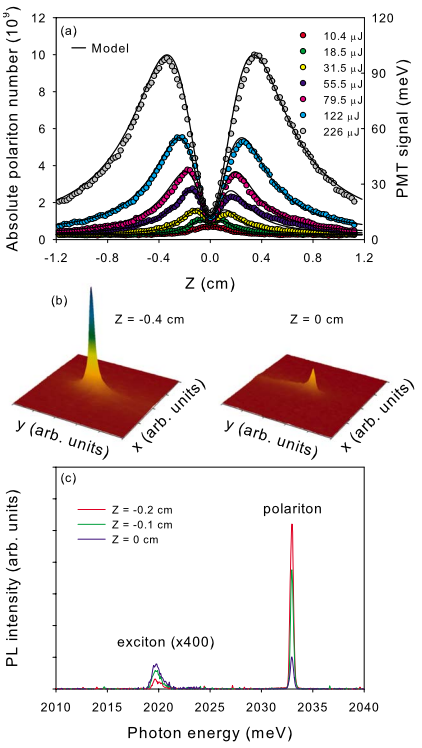

FIG. 2. (Color online) (a) 2ω Z-scan traces for various excitations in the range of 10.4–226 μJ/pulse, fit by the theoretical model. (b) Far-field images of the polariton spatial profiles at Z=−0.4 and 0 cm, and (c) time-integrated PL spectra at Z=−0.2, −0.1, and 0 cm for 122 μJ/pulse.

In order to explain 2ω Z-scan, we now model the population and relaxation dynamics of polaritons. The polariton generation rate G should match the laser absorption profile; $G(\mathbf{r};Z)=-(dI/dz)/2=\beta I^2/2$, where a factor of 1/2 accounts for energy conservation during TPA. The temporal behavior of the local polariton density $n(\mathbf{r};Z,t)$ is described by

$$\frac{dn}{dt} = G(\mathbf{r};Z) - \frac{n}{\tau} - An^2, \tag{3}$$

where τ is the polariton lifetime and A is an Auger coefficient.[7] The analytical solution to Eq. (3) exists and the time-averaged density $n(\mathbf{r};Z)$ is given by[24]

$$n(\mathbf{r};Z) = \frac{\int n(\mathbf{r};Z,t)dt}{\int dt} = \frac{\ln[1+An_0(\mathbf{r};Z)\tau]}{A\tau}, \tag{4}$$

where the initial polariton density is well approximated by $n_0(\mathbf{r};Z)=\{[1+4G(\mathbf{r};Z)A\tau_p^2]^{1/2}-1\}/2A\tau_p$ with the pulse width τ_p=30 ps. While n_0 is essentially $G\tau_p$ at low excitation, it approaches to $(G/A)^{1/2}$ and is limited by fast Auger-like decay during the 30-ps buildup time when $GA\tau_p^2 \gg 1$. To obtain the time-averaged polariton number $N(Z)$ for a given Z, we

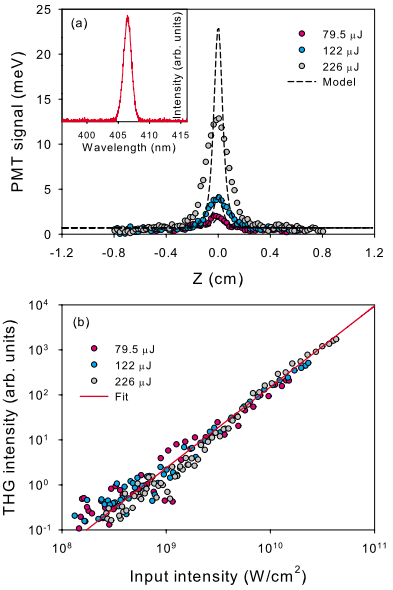

FIG. 3. (Color online) (a) 3ω Z-scan traces for 79.5, 122, and 226 μJ/pulse. The dashed traces are explained in the text. The inset shows the THG spectrum for 226 μJ/pulse. (b) THG intensity obtained from 3ω Z-scan as a function of the input intensity, superimposed by an empirical fit.

numerically integrate $n(\mathbf{r};Z)$ over the sample dimension, $\mathbf{r}$

$$N(Z) = \int n(\mathbf{r};Z)d^3r = \pi\omega^2(Z)\int_0^d n(z;Z)dz. \tag{5}$$

Note that $N(Z)$ contains only two independent fit parameters of τ and A since G is accurately determined with $\beta = 0.217$ cm/GW. The solid traces in Fig. 2(a) show $N(Z)$ using a single fit-parameter set of $\tau = 2$ ns and $A = 0.55 \times 10^{-16}$ cm^3/ns, showing excellent fits to the series of 2ω Z-scan data. A value $\tau = 2$ ns is consistent with that obtained from quantum beat spectroscopy[8] and A is about two times smaller than that reported based on Lyman absorption spectroscopy.[12] Note that the coefficient A for polaritons is more than ten times smaller than that for thermal excitons due to their half-light character.[7,16]

We also confirmed the 2ω Z-scan responses based on direct spectroscopic measurements (see Refs. 14–16 for experimental details). Figure 2(c) shows the time-integrated photoluminescence (PL) spectra recorded at $Z = -0.2$ (red), -0.1 (green), and 0 cm (blue) for 122 μJ/pulse. The sharp lines at 2033 meV arise from the polariton PL and the PL intensities are consistent with the corresponding 2ω Z-scan shown in Fig. 2(a) for respective values of Z. The broad asymmetric PL lines at 2020 meV correspond to the major phonon replica (400× magnified) and essentially reflect the energy distribution of thermal excitons.[25] The Maxwell-Boltzmann fit to the phonon line yields a time-averaged gas temperature of 5 K, which is noticeably higher than the lattice temperature. We found that this PL line is barely detectable for $|Z| > 0.3$ cm but increases in the region of the dip as Z approaches to the focus—see the change in the phonon-

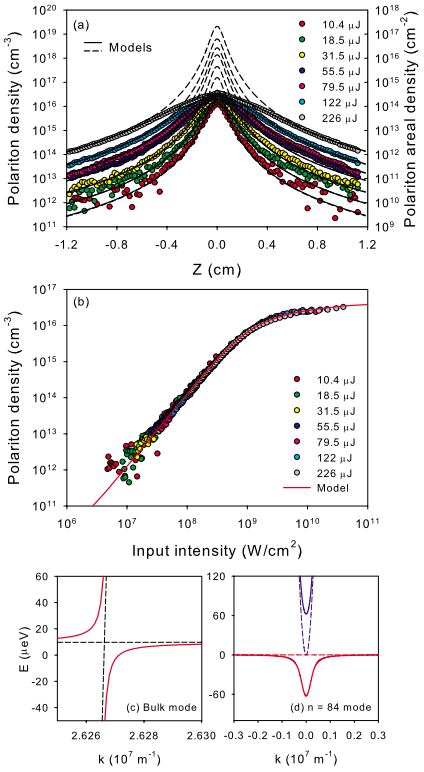

FIG. 4. (Color online) (a) Time-averaged polariton density as a function of Z, superimposed by the models with A (solid traces) and without A (dashed traces). (b) Polariton density as a function of the input intensity, fit by our Auger model. Calculated polariton dispersion for (c) three-dimensional bulk and (d) 10-μm-thick cavity modes in Cu_2O for a (110) direction.

line intensity with Z in Fig. 2(c). This is also consistent with Auger-type decay that produces hot electron-hole pairs subsequently forming thermal excitons.

Since Cu_2O exhibits large $\chi^{(3)}$ responses,[20] we performed 3ω Z-scan to examine THG arising from Re $\chi^{(3)}$. Figure 3(a) displays 3ω Z-scan traces (colored dots) for 79.5, 122, and 226 μJ/pulse, resulting from THG of the input laser, as evidenced by the inset showing the THG signal at $\lambda/3 = 406.5$ nm. We found that 3ω Z-scan responses were very small for lower excitation. Considering a submicron absorption length at 406.5 nm in Cu_2O, however, it is remarkable that measurable THG signals are observed. Since fundamental depletion due to TPA is negligible, the THG field intensity $E_{3\omega}$ as a function of Z is given by[26]

$$E_{3\omega}(Z) = \frac{i3\omega}{2nc}\chi^{(3)}E^3(Z)J_{3\omega}(\Delta kd), \tag{6}$$

where n is the index of refraction for Cu_2O, c is the speed of light, $E(Z) = [I_0(Z)/2nc]^{1/2}$, and $J_{3\omega}(\Delta kd)$ is the phase-matching factor. The dashed traces in Fig. 3(a) are the predicted THG photon counting $[\propto \pi\omega^2(Z)|E_{3\omega}(Z)|^2]$ properly scaled to match the overall data, simply assuming phase matching ($J_{3\omega} = d$) and using $I_0(Z)$ in Eq. (2). While this simple model basically corresponds to a I^3 fit, the observed 3ω Z-scan data reveal a different power dependence, and therefore, are not well explained by these fits. In order to

check the THG power dependence, we plot the corresponding THG intensity (colored dots) $[\propto|E_{3\omega}(Z)|^2]$ in Fig. 3(b) as a function of the input intensity converted from Z using Eq. (2). The red line is an empirical fit to the data with $I^{1.8}$. We believe that this rather unusual power dependence stems from complicated processes involving (i) strong absorption of THG beam that crucially affects phase coherence between the fundamental and THG lights inside Cu_2O and/or (ii) possible contribution due to the generation of higher harmonics. Regardless of detailed THG mechanism, we found that high-density polariton generation is more affected by an Auger-type process rather than THG.

We plot the time-averaged polariton density $n(Z)=N(Z)/\pi\omega^2(Z)d$ (colored dots) in Fig. 4(a) using $N(Z)$ in Fig. 2(a). In our excitation range, the polariton penetration depth is limited by the sample thickness of $d=100$ μm, which is smaller than the two-photon absorption length $(\beta I)^{-1}$. The corresponding areal densities $N(Z)/\pi\omega^2(Z)$ are also plotted in Fig. 4(a). Despite considerable decrease in $N(Z)$ around $Z=0$ in Fig. 2(a), it is important to note that the maximum density still locates at the focus. While the solid traces are our Auger model, the dashed traces correspond to the predicted $n(Z)$ assuming $A=0$, which clearly demonstrates the critical role of the Auger-type effect. The colored dots in Fig. 4(b) correspond to the polariton density as a function of the input intensity, obtained using the same method in Fig. 3(b), superimposed by our model (red curve). It shows that the experimental polariton density strongly saturate s around 3×10^{16} cm^{-3} under high excitation levels. This is more than ten times higher than the maximum thermal exciton density ($\simeq10^{15}$ cm^{-3}),[27] basically due to the suppressed A value by the same amount.

Although the polariton areal densities we have observed in Cu_2O are much higher than the critical BEC density ($\simeq10^9$ cm^{-2}) in the 2D cavity-polariton structures,[4–6] BEC is not expected to arise in practice, since the *absence of a local minimum* precludes condensation [see Fig. 4(c)]; of course such minima have been engineered into the polariton dispersion curves of the microcavities. This limitation might be circumvented by depositing partially transmitting mirrors on opposing sides of a flat platelet of Cu_2O, thereby forming a Fabry-Perot cavity. Figure 4(d) plots the $n=84$ cavity-photon mode for a 10-μm-thick Cu_2O platelet that form a Fabry-Perot cavity (blue dashed curve) sitting just above the bare exciton mode (red dashed curve).[28] (Matching of the mode frequency with the polariton frequency can be achieved by adjusting the propagation direction relative to the plane normal.) Then, the lower polariton branch (red solid curve) would develop a local minimum via quadrupole coupling associated with a very small effective mass ($\simeq10^{-5}m_e$) in which long-lived polaritons can condense.

In conclusion, various nonlinear optical processes have been characterized at the two-photon polariton resonance in Cu_2O using Z-scan. The measured polariton density appears to be high enough for long-lived polariton BEC if cavity confinement is realized in a thin Cu_2O crystal.

This work is supported by the National Science Foundation IGERT under Grant No. 0801685 and the Northwestern Materials Research Center under NSF under Grant No. DMR-0520513.

*Present address: Department of Physics, Applied Physics and Astronomy, The State University of New York at Binghamton, Binghamton, NY 13902, USA; jjoon@binghamton.edu

[1] M. H. Anderson *et al.*, Science **269**, 198 (1995).
[2] K. B. Davis*et al.*, Phys. Rev. Lett. **75**, 3969 (1995).
[3] See, for example, *Bose-Einstein Condensation*, edited by A. Griffin, D. W. Snoke, and S. Stringari (Cambridge University Press, Cambridge, England, 1995).
[4] H. Deng *et al.*, Proc. Natl. Acad. Sci. U.S.A. **100**, 15318 (2003).
[5] J. Kasprzak *et al.*, Nature (London) **443**, 409 (2006).
[6] R. Balili *et al.*, Science **316**, 1007 (2007).
[7] J. I. Jang and J. P. Wolfe, Phys. Rev. B **74**, 045211 (2006) and references therein.
[8] D. Fröhlich *et al.*, Phys. Rev. Lett. **67**, 2343 (1991).
[9] M. Y. Shen *et al.*, Phys. Rev. B **56**, 13066 (1997).
[10] Y. Sun *et al.*, Phys. Rev. B **63**, 125323 (2001).
[11] M. Kubouchi *et al.*, Phys. Rev. Lett. **94**, 016403 (2005).
[12] K. Yoshioka and M. Kuwata-Gonokami, Phys. Rev. B **73**, 081202(R) (2006).
[13] T. Tayagaki *et al.*, Phys. Rev. B **74**, 245127 (2006).
[14] J. I. Jang and J. B. Ketterson, Phys. Rev. B **76**, 155210 (2007).
[15] J. I. Jang *et al.*, Phys. Rev. B **77**, 075201 (2008).
[16] J. I. Jang and J. B. Ketterson, Solid State Commun. **146**, 128 (2008).
[17] T. Ideguchi *et al.*, Phys. Rev. Lett. **100**, 233001 (2008).
[18] J. I. Jang *et al.*, Appl. Phys. Lett. **93**, 121111 (2008).
[19] The polariton concept is not explicitly introduced in Refs. 9–18; however, coherent polaritons are the entity generated under resonant two-photon excitation (see Ref. 15).
[20] S. E. Mani *et al.*, Opt. Lett. **34**, 2817 (2009).
[21] M. Sheik-Bahae *et al.*, IEEE J. Quantum Electron. **26**, 760 (1990).
[22] M. Sheik-Bahae *et al.*, IEEE J. Quantum Electron. **27**, 1296 (1991).
[23] If the sample is infinitely thick, the incident IR photons N should be all absorbed and the number of polaritons generated is simply $N/2$, independent of $I_0(Z)$.
[24] J. I. Jang *et al.*, Phys. Rev. B **74**, 235204 (2006).
[25] M. M. Beg and S. M. Shapiro, Phys. Rev. B **13**, 1728 (1976).
[26] R. W. Boyd, *Nonlinear Optics*, 3rd ed. (Academic Press, San Diego, 2008), p. 119.
[27] K. E. O'Hara and J. P. Wolfe, Phys. Rev. B **62**, 12909 (2000).
[28] A platelet of this size can be achieved by lapping a bulk crystal. Smaller node numbers and large mode spacings would require a thinner sample; a promising technology to make thin films showing sharp exciton lines was reported by P. R. Markworth *et al.*, J. Mater. Res. **16**, 914 (2001). Band gaps could also be engineered by forming a hole array in a thin film that supports waveguide polariton modes.